International Journal of Thermal Sciences 90 (2015) 290–297

Contents lists available at ScienceDirect

International Journal of Thermal Sciences

journal homepage: www.elsevier.com/locate/ijts

# Thermo-fluid analysis of micro pin-fin array cooling configurations for high heat fluxes with a hot spot

Abas Abdoli, Gianni Jimenez, George S. Dulikravich*

*Florida International University, Department of Mechanical and Materials Engineering, MAIDROC Laboratory, Miami, FL 33174, USA*

A R T I C L E I N F O

*Article history:*
Received 23 July 2014
Received in revised form
22 December 2014
Accepted 22 December 2014
Available online

*Keywords:*
Electronics cooling
Micro pin-fin
High heat flux chip
Hot spot
Conjugate heat transfer

A B S T R A C T

Effect of micro pin-fin shapes on cooling of high heat flux electronic chips with a single hot spot was investigated numerically. Hydrothermal performances of different micro pin-fin shapes were evaluated. Circular shape, hydrofoil shape, modified hydrofoil shape, and symmetric convex shape were the cross section shapes used for micro pin-fins. All cooling configurations had the same staggered arrangements for micro pin-fins. An electronic chip with a 2.45 × 2.45 mm footprint having a hot spot of 0.5 × 0.5 mm at its centre was used for simulations. Uniform heat flux of 2000 W cm$^{-2}$ was applied at the hot spot. The rest of the chip was exposed to 1000 W cm$^{-2}$ uniform heat load. The cross section area of the circular shape and hydrofoil shape micro pin-fins was kept the same to have a fair comparison. Convex and hydrofoil shape designs showed significant reduction in the required pumping power as well as the maximum required pressure. In the last case, the height of micro pin-fins was increased from 200 μm to 400 μm to remove 100% of the total heat load *via* convection, and at the same time keep the maximum temperatures within an acceptable range.



## 1. Introduction

Three-dimensional (3-D) integrated circuits (ICs) are believed to be the best way to overcome barriers in inter-connect scaling and keep Moore's law ticking by providing an opportunity for continued higher performance ICs in the semiconductor industry [1]. Smaller size, higher performance, better functionality and lower consumption of power are some of the major advantages of 3-D ICs. On the other hand, increasing demand for removing heat from 3-D ICs has become the major challenge in this field and has constrained their applications. The next generation of the electronic chips is expected to produce heat fluxes up to 500 W cm$^{-2}$ as the background and more than 1000 W cm$^{-2}$ at hot spots [2,3].

Sahu et al. [4] applied a hybrid cooling scheme which combines microfluidic and solid-state cooling techniques in cooling hot spots with the heat flux close to 250 W cm$^{-2}$. In other research, Sahu et al. [5] studied a liquid-thermoelectric hybrid cooling method for hot spots having heat fluxes of more than 600 W cm$^{-2}$. They reported that liquid-thermoelectric hybrid cooling showed better results for higher heat fluxes at hot spots. Abdoli and Dulikravich [6] performed multiobjective optimization for multi-layer straight and branching counterflow microchannel configurations with 67 design variables to maximize heat removal capacity, while minimizing temperature non-uniformity and coolant pumping pressure drop. They also optimized the multi-layer through-flow microchannels for heat fluxes up to 1000 W cm$^{-2}$ [7]. Abdoli et al. [8] also performed a fully 3-D thermal-fluid-stress-deformation analysis for cooling chips with 1000 W cm$^{-2}$ background heat flux and up to 2000 W cm$^{-2}$ heat flux at the hot spot. They reported that multi-floor microchannels are capable of cooling such chips without exceeding the maximum allowable stresses.

Micro pin-fins have shown very promising results in conveying heat from multiple layers to the heat sink [9,10]. Alfieri et al. [11] numerically investigated cooling of 3-D stacked chips with 50 W cm$^{-2}$ background and 125 W cm$^{-2}$ hot spot heat fluxes. They studied the influence and implications of the integrated water cooling, micro pin-fins distribution and sizes also influence temperature of hot spots. Alfieri et al. [12] in another research modelled vortex shedding in water cooling of 3-D integrated electronics. Zhang et al. [13,14] experimentally investigated effects of silicon micro pin-fin heat sink with integrated TSVs in cooling high power chips. Dembla et al. [15] also studied the fine pitch TSV integration in silicon micro pin-fin heat sinks for 3D ICs with 100 W cm$^{-2}$ heat load.

* Corresponding author.
*E-mail addresses:* aabdo004@fiu.edu (A. Abdoli), gjime006@fiu.edu (G. Jimenez), dulikrav@fiu.edu (G.S. Dulikravich).

http://dx.doi.org/10.1016/j.ijthermalsci.2014.12.021
1290-0729/

In the present work, fully 3-D conjugate thermo-fluid analysis of micro pin-fins was performed for four geometrically different cross sections micro pin-fins: a conventional circular shape, a hydrofoil shape, a modified hydrofoil shape and a symmetric convex lens shape. In Sections 2–5, results of these four different designs with the same boundary conditions are presented. Section 6 shows the results of symmetric convex lens micro pin-fins with adiabatic bottom surface. In the last cooling case, height of the micro pin-fins was doubled to reduce the maximum temperature at the top and bottom surfaces.

## 2. Case 1: micro pin-fins with circular cross section

An array of cylindrical shape micro pin-fins was virtually designed for cooling an electronic chip with dimensions of 2.45 × 2.45 × 0.28 mm. Fig. 1 shows the staggered arrangement of the micro pin-fins and the spacing between them. A hot spot with dimensions of 0.5 × 0.5 mm was located at the centre of the chip. A total of eleven crossflow rows of micro pin-fins can be observed in Fig. 1. Six of these rows included nine micro pin-fins and five of them included eight micro pin-fins. The reason for staggered arrangement of micro pin-fins was to enhance the convection heat transfer [16]. Fig. 1b shows that centre-to-centre distance between micro pin-fins was 250 μm. The side walls thickness was 60 μm. The bottom and top walls were 40 μm thick. Diameter of each micro pin-fin was 173 μm. Most of the geometric arrangements and sizes were adopted from Refs. [13–15]. Material for substrate and micro pin-fins was assumed to be Silicon and coolant was water.

All 3D conjugate heat transfer simulations presented in this paper were carried out using ANSYS Fluent® software [17]. ANSYS meshing® was adopted as the computational grid generation tool. Considering the geometry and physics of the problem, all cases were eligible for symmetric assumption. Therefore, all geometries were cut in half in the streamwise direction to reduce computational costs noticeably. Standard k–ε turbulent model was used in all cases due to its stability, good convergence rate and relatively low required memory. A hybrid mesh with viscous sub-layer refinement next to solid surfaces was used for discretization of the solution domain. The viscous sub-layer mesh had the minimum height of 1 μm with growth rate of 1.2. Mesh independency was reached for a mesh with 6,900,000 cells. A sample of the hybrid mesh is presented in Section 4 which has sharper edges.

Inlet averaged speed and temperature of water were set to 2.0 m $s^{-1}$ and 26.85 °C, respectively. The outlet gauge pressure was set to 20 kPa. The temperature gradient normal to the outlet was set to zero. Coolant boundary conditions were kept the same for all cases. The following are the applied boundary conditions for the solid domain:

**Table 1**
Case 1 – micro pin-fins with circular cross section: geometric parameters.

| Design parameter | Value | Design parameter | Value |
|---|---|---|---|
| Number of micro pin-fins | 94 | Total wetted area of micro pin-fins ($mm^2$) | 10.23 |
| Total cross section area of all micro pin-fins ($mm^2$) | 2.215 | Micro pin-fin area ratio (wetted area/cross section area) | 4.62 |

1. Constant input heat flux of 2000 W $cm^{-2}$ for the hot spot on the top surface,
2. Constant input heat flux of 1000 W $cm^{-2}$ for background on the top surface,
3. Constant temperature of 26.85 °C on the bottom surface,
4. Thermally insulated side walls.

The bottom surface temperature was assumed to be close to the room temperature as in an ideal situation. These thermal boundary conditions were also kept the same for the next three cases. In the last two cooling cases, the thermally insulated boundary condition was enforced at the bottom surface as in a worst-case scenario.

Some of geometric parameters of micro pin-fins with circular cross section are given in Table 1. Total number of micro pin-fins was 94. The ratio of the total wetted area (fluid contact area) of this arrangement of micro pin-fins to the total cross sections area (chip contact area with one micro pin-fin) in this case was 4.62.

Fig. 2 shows thermo-fluid analysis results for this case. Temperature distribution in the entire half of the configuration is shown in Fig. 2a. The coolant flow direction was in the x-direction. The maximum temperature in this case was 78.95 °C which occurred at the hot spot. Higher temperature region can also be observed near the coolant outlet. Fig. 2b illustrates the temperature variations in micro pin-fins in one half of the configuration. Micro pin-fins under the hot spot had the maximum temperature. Also, higher temperatures can be seen near the flow exit. Fig. 2c shows the heat flux distribution normal to the bottom surface. This is an indication of the heat removed from the chip by conduction. As this figure illustrates, conduction heat transferred portion was increased in the streamwise direction. This is due to water temperature increase in this direction, which resulted in a decrease in convection heat transfer and an increase in conduction heat transfer. The maximum conduction occurred under the hot spot. This shows that the convection heat transfer *via* water was not

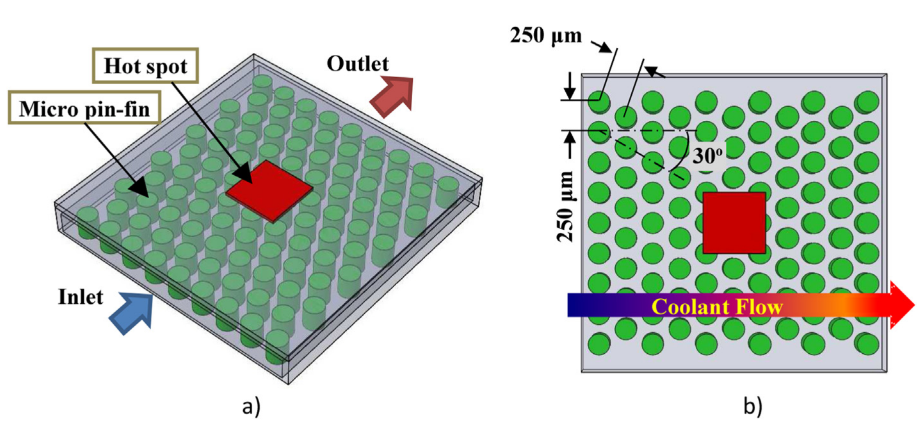


**Fig. 1.** Case 1 – cylindrical micro pin-fins with circular cross section: a) 3-D view, and b) top view with dimensions.

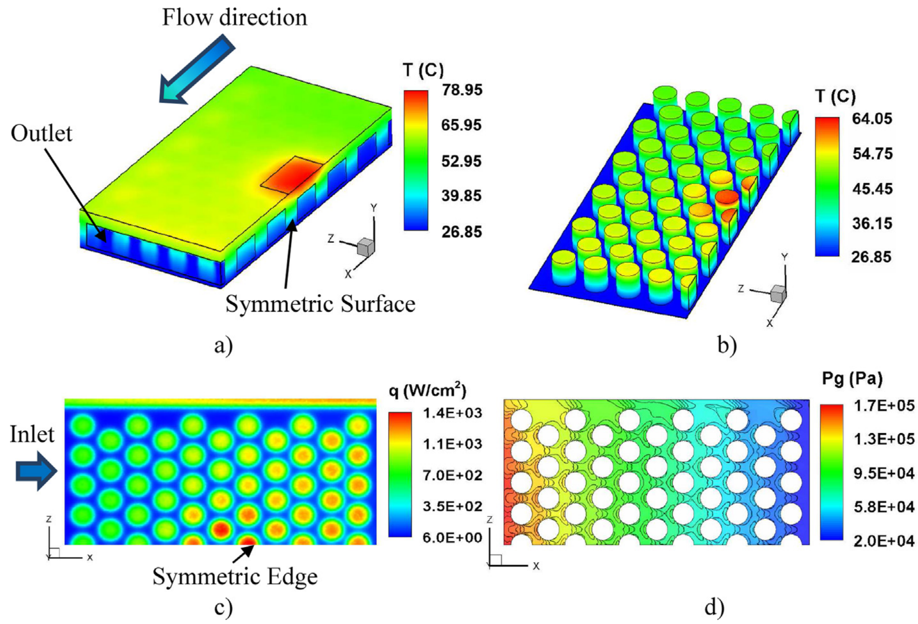


**Fig. 2.** Case 1 – thermo-fluid conjugate analysis results: a) temperature distribution of one half of the chip, b) temperature distribution of half of micro pin-fins, c) heat flux normal to the bottom surface, and d) gauge pressure distribution with isobar lines.

capable of removing all the heat applied at the hot spot. Gauge pressure distribution with isobar lines is shown in Fig. 2d. The maximum of the inlet gauge pressure was 1.7 kPa. Higher pressure can be observed in front of micro pin-fins. Large separation regions behind circular cross section micro pin-fins caused a significant reduction in convection heat transfer in these regions.

To better examine the performance of this shape of micro pin-fins, some of the output parameters are presented in Table 2. Total amount of applied heat on the chip was 62.525 W, where 33.809 W of it was removed *via* convection, and 28.716 W was removed *via* conduction from the bottom surface. This means that water was capable of removing 54.07% of the applied heat in this cooling case. Pumping power to overcome the pressure drop between the inlet and outlet was 0.131 W. The average inlet pressure was used in pumping power calculation.

## 3. Case 2: micro pin-fins with hydrofoil cross section

The major drawback of micro pin-fins with circular cross section shape is the flow separation behind each such pin-fin. This increases the required inlet pressure and at the same time decreases the convection heat transfer. Therefore, a shape resembling a NACA0060 symmetric airfoil was used as a cross section instead of a circular shape to create micro pin-fins. Such aerodynamic/hydrodynamic cross section shape was expected to provide better hydrothermal efficiency as a potential candidate to replace circular cross section shape micro pin-fins in a closely packed array, which is different than in a sparsely populated array [18].

Table 3 shows some of the geometric parameters for hydrofoil micro pin-fins where the number of micro pin-fins and their cross section areas were kept the same as in the case of circular cross section micro pin-fins. However, since the height of micro pin-fins remained the same in all designs, variation in fluid contact areas between Case 1 and Case 2 was inevitable. The micro pin-fins staggered arrangement and the centre-to-centre distances between micro pin-fins were kept the same as in the circular cross section pin-fins design. Total number of computational cells to reach the mesh independency was around 7,700,000 for this configuration.

Fig. 3 shows the simulation results for an array of micro pin-fins with symmetric hydrofoil cross sections. The maximum temperature at the hot spot was 77.15 °C, which was 1.80 °C less than in Case 1. The maximum temperature of the micro pin-fins in this case was 1.70 °C less than in Case 1. The maximum conduction heat transfer in this case was 10% lower than in Case 1. The most significant enhancement was 23.5% reduction of the maximum pressure (gauge) which went from 1.7 kPa in Case 1 to 1.3 kPa in Case 2.

Table 4 demonstrates output parameters for hydrofoil cross section shape array of the micro pin-fins. It can be observed that hydrofoil shape micro pin-fins increased the convection heat transfer portion. The ratio of convectively removed over total input heat in this design was 3.2% higher than in Case 1. By increasing the fluid contact area, it could be expected to have higher pressure drop. However, in this design, pumping power was 30.4% lower than in Case 1. This indicates the importance of separation flow control for such cooling configurations.

**Table 2**
Case 1 – micro pin-fins with circular cross section: computational results.

| Output parameter | Value | Output parameter | Value |
|---|---|---|---|
| Convection heat removed (W) | 33.809 | Pumping power (W) | 0.131 |
| Conduction heat removed (W) | 28.716 | Average temp. of the hot spot (°C) | 74.96 |
| Convection/heat load (%) | 54.07 | Average temp. of rest of the chip (°C) | 61.30 |

**Table 3**
Case 2 – micro pin-fins with hydrofoil cross section: geometric parameters.

| Design parameter | Value | Design parameter | Value |
|---|---|---|---|
| Number of micro pin-fins | 94 | Total wetted area of micro pin-fins ($mm^2$) | 11.151 |
| Total cross section area of all micro pin-fins ($mm^2$) | 2.215 | Micro pin-fin area ratio (wetted area/cross section area) | 5.03 |

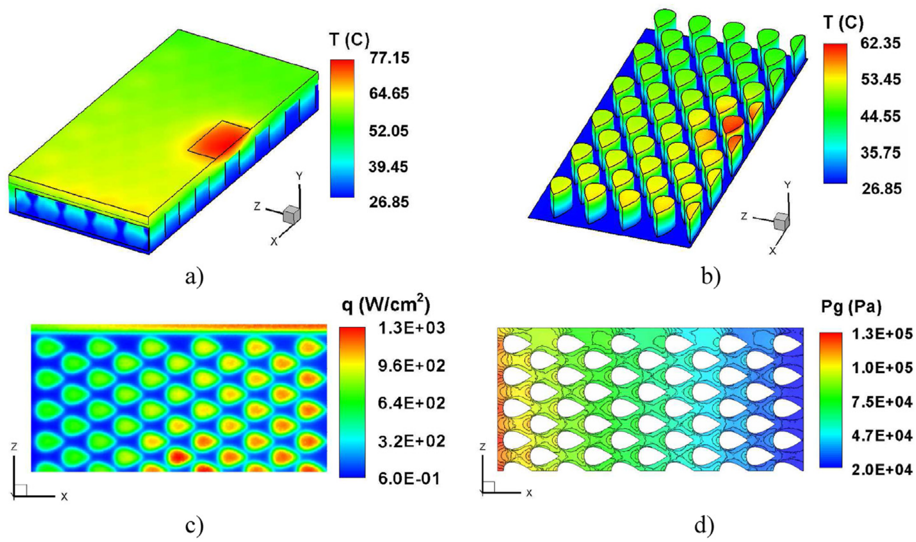


**Fig. 3.** Case 2 – thermo-fluid conjugate analysis results: a) temperature distribution on one half of the chip, b) temperature distribution on half of micro pin-fins, c) heat flux normal to the bottom surface, and d) gauge pressure distribution with isobar lines.

## 4. Case 3: micro pin-fins with modified hydrofoil cross section

The main objective of the modified hydrofoil micro pin-fin design presented in this section was to decrease the maximum temperature of the hot spot and near the outlet. Thus, larger size hydrofoil shape micro pin-fins were used under the hot spot. Also, at the outlet the shapes of micro pin-fins were modified to increase conduction heat transfer and prevent flow separation and reverse flow. In addition, half-hydrofoil shape micro pin-fins were attached to the side wall in the streamwise direction to enhance the heat transfer. Mesh independent results in this case were obtained for the total number of computational cells around 7,000,000.

Total number of micro pin-fins in Case 3 was larger than in previous cases (see Table 5). Total solid contact (micro pin-fins cross section) area in this case was 12.1% larger than in Case 2. Total fluid contact area was 18.3% larger than in Case 1 and 8.5% larger than in Case 2. This table also declares three different ratios for the fluid contact area over solid contact area in Case 3.

As Fig. 4a illustrates, the maximum temperature in this case was 72.75 °C which was 6.4 °C and 4.4 °C less than in Case 1 and Case 2, respectively. Lower temperatures can also be observed near the outlet compared to previous cases. The maximum conduction heat transfer was also decreased. However, higher conduction heat transfer was calculated in this case. This was due to the larger total micro pin-fins contact area with the chip. The maximum pressure in this case was 11.8% lower than in Case 1 and 13.3% higher than in Case 2. This increase in the maximum pressure was mainly because of the larger fluid contact area.

Table 6 shows that the ratio of convectively removed heat over total heat load in this case was 1.3% and 4.5% less than cylindrical and hydrofoil shape micro pin-fins, respectively. Pumping power calculated for this case was 13.0% less than in Case 1 and 25.3% higher than in Case 2.

## 5. Case 4: micro pin-fins with symmetric convex cross section

In Case 4, symmetric convex (lense) shape was used as cross section for all micro pin-fins. The same concept was used for micro pin-fin sizes as in Case 3. That is, larger size convex cross section shapes of micro pin-fins were used under the hot spot, and the modified convex shapes were used at the outlet. Total number of computational cells in this case was around 7,800,000. Fig. 5 shows the cut-away view of the hybrid mesh with an enlarged view close to the solid walls.

Table 7 shows geometric parameters for the Case 4. Total number of micro pin-fins in this case was the same as in Case 3. Total solid contact (micro pin-fins cross section area) in this case was 4.2% larger than in Case 3. Total fluid contact area was 6.0% larger than in Case 3. Unlike in the case of modified hydrofoil shapes, the ratio of the fluid contact area over cross section area under the hot spot was higher than in the rest of the Case 4 configuration. Also, this ratio for the micro pin-fins near the outlet was higher than for the rest of the chip.

Fig. 6 illustrates the thermo-fluid analysis results for Case 4. The maximum temperature of the entire design in this case was 73.35 °C, which was only 0.60 °C higher than in the modified hydrofoil design. However, larger temperatures around the hot spot and near the outlet can be observed compared to Case 3. The maximum conduction heat transfer in Case 4 was slightly higher than in Case 3. The maximum inlet pressure in Case 4 was 41.2%

**Table 4**
Case 2 – micro pin-fins with hydrofoil cross section: computational results.

| Output parameter | Value | Output parameter | Value |
|---|---|---|---|
| Convection heat removed (W) | 35.802 | Pumping power (W) | 0.091 |
| Conduction heat removed (W) | 26.723 | Average temp. of the hot spot (°C) | 73.08 |
| Convection/heat load (%) | 57.26 | Average temp. of rest of the chip (°C) | 60.31 |

**Table 5**
Case 3 – micro pin-fins with modified hydrofoil cross sections: geometric parameters.

| Design parameter | Value | Design parameter | | Value |
|---|---|---|---|---|
| Number of micro pin-fins | 99 | Total wetted area of micro pin-fins ($mm^2$) | | 12.097 |
| Total micro pin-fins cross section area ($mm^2$) | 2.483 | Micro pin-fin area ratio (wetted area/cross section area) | Under hot spot | 4.42 |
| | | | At the outlet | 4.23 |
| | | | Rest of the chip | 5.03 |

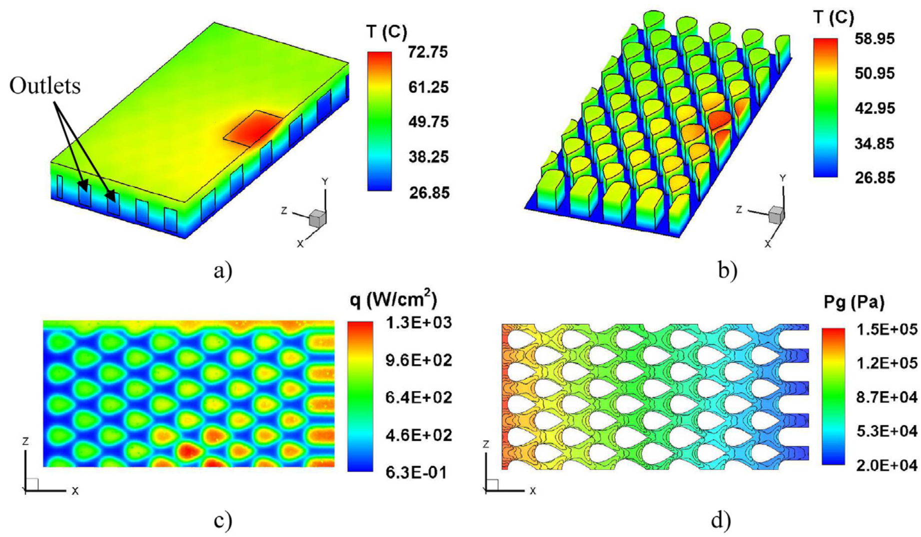


**Fig. 4.** Case 3 – thermo-fluid conjugate analysis results: a) temperature distribution on one half of the chip, b) temperature distribution of half of micro pin-fins, c) heat flux normal to the bottom surface, and d) gauge pressure distribution with isobar lines.

lower than in Case 1, 23.1% lower than in Case 2 and 33.3% lower than in Case 3.

As Table 8 demonstrates, the ratio of convectively removed heat over total heat load in this case was increased 1.3% compared to the modified hydrofoil micro pin-fins case. The average temperature at the hot spot and rest of the chip in this case were 0.72 °C and 1.73 °C less, respectively, than in Case 3. Lower required pumping power was the main advantage of the convex design over the modified hydrofoil design. As Table 8 shows, the required pumping power for this case was 0.069 W, which is 39.5% lower than the required pumping power in the modified hydrofoil micro pin-fin design (Case 3).

## 6. Case 5: micro pin-fins with symmetric convex cross section and insulated bottom surface

Results of the previous case showed that 54.04% of the heat load was removed by water. However, one of the main objectives of such electronic cooling systems is to remove the entire heat load *via* convection heat transfer. Thus, for the simulation presented in this section (Case 5), the bottom surface boundary condition was changed from the constant temperature of 26.85 °C to a thermally insulated surface. This means that all external solid surfaces became thermally insulated, except for the chip surface (top surface). This way, the entire applied heat load will be removed by the coolant. In this case the maximum temperature became the output of interest by which the cooling capability of the micro pin-fin cooling design was measured.

Consequently, the maximum temperature in Case 5 (Fig. 7a) increased to 81.3 °C which is 7.95 °C higher than in Case 4. The temperature distribution of the bottom surface is shown in Fig. 7b. The maximum temperature on this surface was 56 °C. The maximum and average temperature of water was 70.61 °C located close to the hot surface. The average outlet water temperature was 44.77 °C.

Table 9 presents more simulation results. The average temperature of the bottom surface was 43.6 °C. The average temperature of the hot spot and the rest of the chip in Case 5 were 77.77 °C and 68.19 °C, respectively. Pumping power was the same as the one shown in Table 8 (Case 4).

## 7. Case 6: taller micro pin-fins with symmetric convex cross section and insulated bottom surface

Based on the results presented in previous sections, it can be concluded that micro pin-fins with 200 μm height were not able to remove the applied thermal load efficiently using the specified coolant inlet temperature and velocity. In real application, especially in a 3-D stack of chips, it is required to remove the entire applied heat load *via* convection heat transfer without exceeding an acceptable maximum temperature. In this section, taller (400 μm) pin-fins with doubly convex symmetric cross sections were used to enhance the convection heat transfer. The same boundary conditions were applied as in the previous case (Case 5). The total fluid contact area of micro pin-fins in this case was doubled, but the total solid contact area remained the same as in the convex shape micro pin-fin design (Case 4). The mesh parameters were also the same as those in Case 4. Mesh convergence in Case 6 was obtained for a mesh size of 13,000,000 cells.

**Table 6**
Case 3 – micro pin-fins with modified hydrofoil cross sections: computational results.

| Output parameter | Value | Output parameter | Value |
|---|---|---|---|
| Convection heat removed (W) | 32.976 | Pumping power (W) | 0.114 |
| Conduction heat removed (W) | 29.549 | Average temp. of the hot spot (°C) | 69.35 |
| Convection/heat load (%) | 52.74 | Average temp. of rest of the chip (°C) | 58.33 |

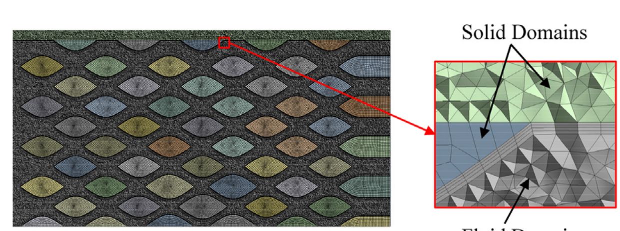


**Fig. 5.** Case 4 – cut away view of the hybrid computational mesh with an enlarged view.

**Table 7**
Case 4 – micro pin-fins with symmetric convex cross sections: geometric parameters.

| Design parameter | Value | Design parameter | | Value |
|---|---|---|---|---|
| Number of micro pin-fins | 99 | Total wetted area of micro pin-fins ($mm^2$) | | 12.819 |
| Total cross section area of all micro pin-fins ($mm^2$) | 2.384 | Micro pin-fin area ratio (wetted area/cross section area) | Under hot spot | 5.58 |
| | | | At the outlet | 4.86 |
| | | | Rest of the chip | 4.60 |

**Table 8**
Case 4 – micro pin-fins with symmetric convex cross sections: computational results.

| Output parameter | Value | Output parameter | Value |
|---|---|---|---|
| Convection heat removed (W) | 33.816 | Pumping power (W) | 0.069 |
| Conduction heat removed (W) | 28.709 | Average temp. of the hot spot (°C) | 70.07 |
| Convection/heat load (%) | 54.08 | Average temp. of rest of the chip (°C) | 60.06 |

Fig. 8a shows that the maximum temperature in Case 6 was 78.9 °C, which is 2.4 °C lower than in Case 5 with 200 μm high convex cross section micro pin-fins. A non-uniform temperature distribution can be observed on the bottom surface (Fig. 8b) with the maximum value of 40.8 °C which was 15.2 °C less than in Case 5. It was located downstream from the hot spot. The average temperature of the bottom surface was 32.3 °C (Table 10).

As Table 10 shows, the average temperature of the hot spot and the rest of the chip were 75.08 °C and 64.65 °C, respectively. Pumping power was two times higher than in Case 5.

## 8. Discussion

The aim of this section is to present a comprehensive discussion based on the fully 3D conjugate thermo-fluid analyses results and provide some useful guidelines for future research, especially for multi-objective design optimization of such cooling configurations. The following are the itemized discussions:

1. In micro pin-fin cooling configuration, flow control has a crucial role in reducing the pumping power and enhancing convection heat transfer. The major disadvantage of classical circular cross section shape micro pin-fins is flow separation which leads to lower convection heat transfer and higher pumping power requirement.
2. Hydrofoil cross section shape micro pin-fins performed better in reducing the flow separation. Thereby, the pumping power was reduced by 30.4% and the ratio of convection over total heat was increased by 3.2% compared to micro pin-fins with circular cross section shape and the same total cross section area. In this research, inlet average velocity and mass flow rate of the coolant were kept constant for all cases. As a result of it, the inlet cross section area and micro pin-fins height (except for Case 6) remained constant in all cases. This led to an inevitable variation between the total fluid contact area of circular cross section micro pin-fins and hydrofoil cross section micro pin-fins. Larger fluid contact area can increase the convection heat transfer as well as pumping power to overcome viscous losses. However, it was shown that hydrofoil shape required much lower pumping power, despite having larger fluid contact areas. This indicated that the flow separation effect was significant, and had large influence on the required pumping power.
3. Modified hydrofoil shape micro pin-fins design can be considered as the first step in optimization path and will help to select the proper design variables. Based on its results, the following can be concluded for a constant inlet velocity and mass flow rate:
   a. To decrease the maximum temperature at hot spots, larger cross section area micro pin-fins are required under the hot spot so that ratio of conduction over convection (micro pin-fin cross section area over fluid contact area) has to be increased. However, heat fluxes well above 2000 W $cm^{-2}$ at hot spot, and smaller size hot spots are the main challenges for the micro pin-fin designs. One solution can be to include more copper *vias* in micro pin-fins under the hot spot to enhance the conduction heat transfer, or to use a material with high thermal conductivity under the hot spot to improve heat conduction vertically from the hot spot. Additional possibility would be to use very high thermal

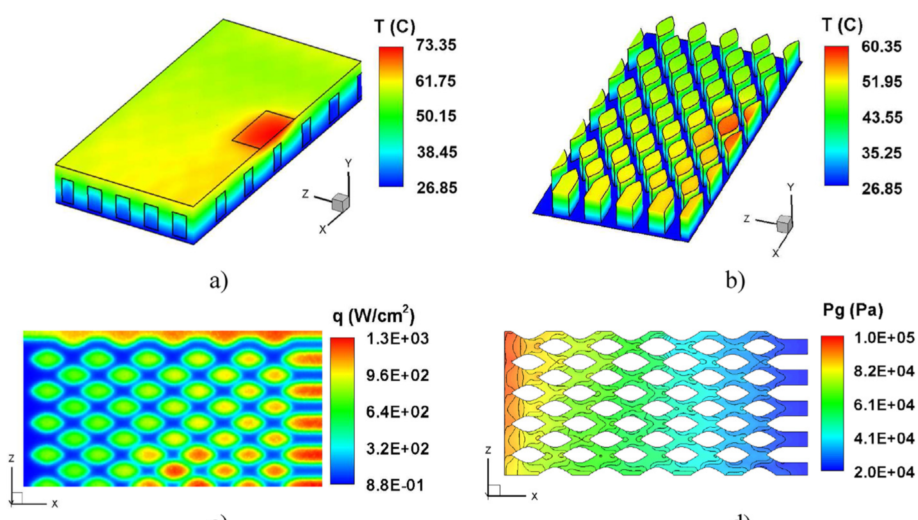


**Fig. 6.** Case 4 – thermo-fluid conjugate analysis results: a) temperature distribution on one half of the chip, b) temperature distribution of half of micro pin-fins, c) heat flux normal to the bottom surface, and d) gauge pressure distribution with isobar lines.

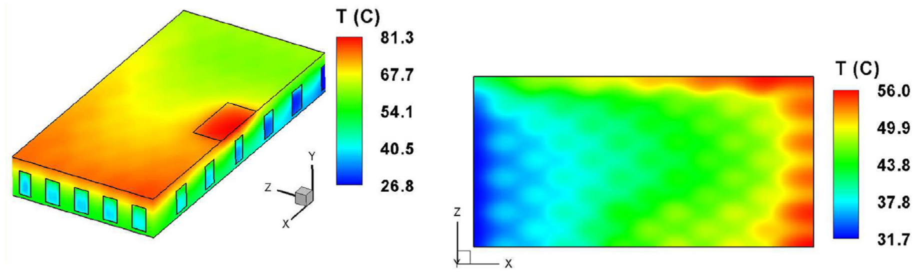


**Fig. 7.** Case 5 – thermo-fluid conjugate analysis results: a) temperature distribution on one half of the chip, and b) temperature distribution on half of the bottom surface.

conductivity thin film coating of the hot surface thus spreading the hot spot heat over a larger portion of the hot surface area.

b. As coolant moves toward the outlet, its temperature increases and convection heat transfer decreases. To compensate for this, micro pin-fins should have larger cross section areas to increase the conduction heat transfer, thereby decreasing the maximum temperature near the outlet. It should also be mentioned that the ratio of fluid contact area over cross section area for micro pin-fins needs to be differentiated at least for three regions: under the hot spot, region near the outlet and rest of the chip.

4. In Section 5, a symmetric convex lens shape was proposed for micro pin-fins cross section. This design required a significantly smaller pumping power compared to other cases. The required pumping power for this case was 47.3% less than for the micro pin-fins with circular cross section, 24.2% less than for the hydrofoil micro pin-fin design and 39.5% less than for the modified hydrofoil micro pin-fin design. The maximum temperature at the hot spot was 5.6 °C less than in circular cross section micro pin-fin design, 3.5 °C less than in the hydrofoil micro pin-fin design and only 0.6 °C higher than in the modified hydrofoil micro pin-fin design. This indicates that the symmetric convex design was the best shape for micro pin-fins, that is, a hydrofoil shape with minimum size flow stagnation regions.
5. Insulated boundary condition was applied at the bottom surface to simulate the worst-case scenario. Results showed maximum temperatures of 81.3 °C and 56 °C at the hot spot and the bottom surface, respectively. The heat transfer efficiency of the micro pin-fins can be enhanced by increasing the inlet mass flow rate of the coolant. However, this will increase the required pumping power, maximum pressure and size of the design. The maximum required pressure is a crucial parameter from the manufacturing point of view. Higher pressure will also increase the risk of coolant leakage. In Section 6, where a micro pin-fin design with double-height (400 μm) was studied, pumping power was doubled, but the maximum pressure remained the same as in case with 200 μm height micro pin-fins (Case 5). This double-height micro pin-fin design (Case 6) decreased the maximum temperature of the bottom surface by 15.2 °C compared to Case 5. However, a multi-objective optimization study is required to find the optimal convex shape micro pin-fin design with maximum heat removal capacity and minimum required pumping power. Height and cross section area of the micro pin-fins and coolant inlet velocity can be design variables for such a study. The maximum allowable temperatures on the top and bottom surfaces can be the two constraints.

## 9. Conclusions

Thermo-fluid analysis was performed for six different micro pin-fin cooling cases. Hydrofoil shape micro pin-fin design showed 30.4% reduction in pumping power and 3.2% increase in the ratio of convection over total heat load compared to conventional circular cross section shape micro pin-fin design. Modified hydrofoil shape micro pin-fin design was able to decrease the maximum temperature by 6.4 °C compared to the circular cross section design. Convex shape micro pin-fin design reduced the pumping power by 47.3% compared to the circular cross section shape design. In the last two simulations, the bottom surface was assumed to be an insulated surface. Thus, in these two cases, all the applied amount of heat was removed by the coolant thus simulating the cooling requirement for stacks of electronic chips. Tall convex cross section micro pin-fin design (Case 6) reduced the maximum temperature of the bottom surface significantly. The maximum temperature in this case had a fairly good value of 78.9 °C. It should be pointed out that all these results (Table 11) were obtained without any mathematical optimization. In future research, multi-objective optimization methods should be applied to find optimal values for geometric parameters defining convex micro pin-fin shapes, sizes and locations that will simultaneously maximize the heat removal efficiency, minimize pumping power, minimize the maximum required pressure and minimize the maximum temperature at the hot spot. The maximum allowable temperature can be set as the constraint.

**Table 9**
Case 5 – micro pin-fins with symmetric convex cross sections (thermally insulated bottom surface of the electronic package): computational results.

| Output parameter | Value | Output parameter | Value |
|---|---|---|---|
| Convection heat removed (W) | 62.52 | Ave. temp. of the bottom surface (°C) | 43.6 |
| Conduction heat removed (W) | 0 | Ave. temp. of the hot spot (°C) | 77.77 |
| Convection/heat load (%) | 100 | Ave. temp. of the rest of chip (°C) | 68.19 |

**Table 10**
Case 6 – taller micro pin-fins with symmetric convex cross sections (thermally insulated bottom surface of the electronic package): computational results.

| Output parameter | Value | Output parameter | Value |
|---|---|---|---|
| Convection heat removed (W) | 62.525 | Ave. temp. of the bottom surface (°C) | 32.3 |
| Conduction heat removed (W) | 0 | Ave. temp. of the hot spot (°C) | 75.08 |
| Convection/heat load (%) | 100 | Ave. temp. of the rest of chip (°C) | 64.65 |

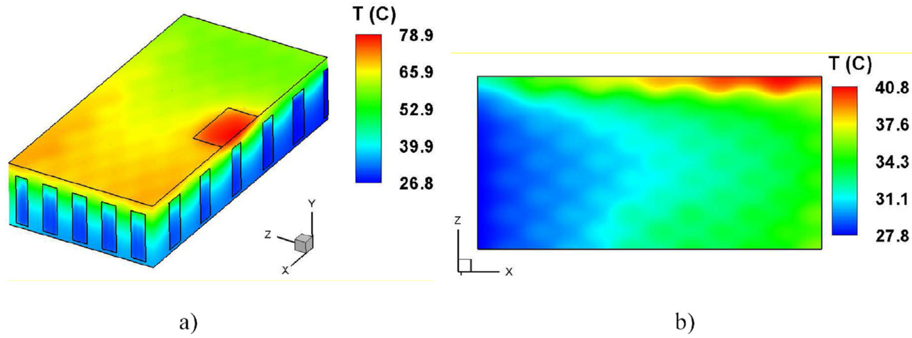


**Fig. 8.** Case 6 – thermo-fluid conjugate analysis results for taller pin-fins: a) temperature distribution on one half of the chip, and b) temperature distribution of half of the bottom surface.

**Table 11**
Summary of major performance parameters.

| Parameter | Case 1 | Case 2 | Case 3 | Case 4 | Case 5 | Case 6 |
|---|---|---|---|---|---|---|
| Heat removed by convection/ total heat load (%) | 54.07 | 57.26 | 52.74 | 54.08 | 100.00 | 100.00 |
| Pumping power (W) | 0.131 | 0.091 | 0.114 | 0.069 | 0.069 | 0.14 |
| Maximum temp. of hot spot (°C) | 78.95 | 77.15 | 72.75 | 73.35 | 81.3 | 78.9 |
| Average temp of hot surface (°C) | 74.96 | 73.08 | 69.35 | 70.07 | 77.77 | 75.08 |

## Acknowledgements

Authors are grateful for partial financial support of this research provided by DARPA via GaTech in the framework of ICECool project. The authors also gratefully acknowledge the FIU Instructional and Research Computing Center for providing HPC resources in conducting this project. The lead author would like to acknowledge the financial support of the Florida International University Dissertation Year Fellowship.

## References

[1] H. Lee, K. Chakrabarty, Test challenges for 3D integrated circuits, IEEE Des. Test (99) (2009), http://dx.doi.org/10.1109/MDT.2009.102.
[2] A. Bar-Cohen, Gen-3 thermal management technology: role of microchannels and nanostructures in an embedded cooling paradigm, J. Nanotechnol. Eng. Med. 4 (2) (2013) 020907, http://dx.doi.org/10.1115/1.4023898. Paper No: NANO-12–1130.
[3] V. Sahu, Y. Joshi, A. Fedorov, Hybrid solid state/fluidic cooling for hot spot removal, Nanoscale Microscale Thermophys. Eng. 13 (2009) 135–150.
[4] V. Sahu, Y.K. Joshi, A.G. Fedorov, Experimental investigation of hotspot removal using superlattice cooler, in: Thermal and Thermomechanical Phenomena in Electronic Systems (ITherm), 12th IEEE Intersociety Conference, Las Vegas, NV, 2–5 June, 2010, pp. 1–8.
[5] V. Sahu, A.G. Fedorov, Y. Joshi, K. Yazawa, A. Ziabari, A. Shakouri, Energy efficient liquid–thermoelectric hybrid cooling for hot-spot removal, in: Semiconductor Thermal Measurement and Management Symposium (SEMI-THERM), 28th Annual IEEE, San Jose, CA, 18–22 March, 2012, pp. 330–348.
[6] A. Abdoli, G.S. Dulikravich, Multi-objective design optimization of multi-floor, branching, counterflow micro heat exchangers, paper HT2013-17738ASME Heat Transfer Conference, Minneapolis, MN, July 14–19 (2013), ASME J. Heat Transfer vol. 136 (Oct. 2014) 101801-1–101801-101810.
[7] A. Abdoli, G.S. Dulikravich, Optimized multi-floor throughflow micro heat exchangers, Int. J. Therm. Sci. 78 (April 2014) 111–123.
[8] A. Abdoli, G.S. Dulikravich, G. Vasquez, S. Rastkar, Thermo-fluid-stress analysis in microchannels cooling of electronics with hot spots, in: N. Massarotti, P. Nithiarasu, B. Sarler (Eds.), ThermaComp2014, June 2–4 2014, pp. 495–498. Lake Bled, Slovenia.
[9] J. Burns, TSV-based 3D integration, in: A. Papanikolaou, D. Soudris, R. Radojcic (Eds.), Three Dimensional System Integration, Springer, Nov. 2010, pp. 13–22.
[10] Z. Liu, S. Swarup, S.X.-D. Tan, Compact lateral thermal resistance modeling and characterization for TSV and TSV array, in: 2013 IEEE/ACM International Conference on Computer-aided Design (ICCAD), 18–21 November 2013, pp. 275–280, http://dx.doi.org/10.1109/ICCAD.2013.6691132.
[11] F. Alfieri, S. Gianini, M.K. Tiwari, T. Brunschwiler, B. Michel, D. Poulikakos, Computational modeling of hot-spot identification and control in 3-D stacked chips with integrated cooling, Numer. Heat Transfer Part A 65 (2014) 201–215.
[12] F. Alfieri, M.K. Tiwari, A. Renfer, T. Brunschwiler, B. Michel, D. Poulikakos, Computational modeling of vortex shedding in water cooling of 3D integrated electronics, Int. J. Heat Fluid Flow 44 (2013) 745–755.
[13] Y. Zhang, A. Dembla, M.S. Bakir, Silicon micropin-fin heat sink with integrated TSVs for 3-D ICs: tradeoff analysis and experimental testing, IEEE Trans. Compon. Packag. Manuf. Technol. 3 (11) (2013) 1842–1850.
[14] Y. Zhang, L. Zheng, M.S. Bakir, 3-D stacked tier-specific microfluidic cooling for heterogeneous 3-D ICs, IEEE Trans. Compon. Packag. Manuf. Technol. 3 (11) (2013) 1811–1819.
[15] A. Dembla, Y. Zhang, M.S. Bakir, Fine pitch TSV integration in silicon micropin-fin heat sinks for 3D ICs, in: Interconnect Technology Conference (IITC), 2012 IEEE International, 4–6 June 2012, pp. 1–3, http://dx.doi.org/10.1109/IITC.2012.6251587.
[16] A. Koşar, Y. Peles, Thermal-hydraulic performance of MEMS-based pin fin heat sink, ASME J. Heat Transfer 128 (2) (2005) 121–131, http://dx.doi.org/10.1115/1.2137760.
[17] ANSYS Fluent, http://ansys.com/Products/Simulation+Technology/Fluid+Dynamics.
[18] S. Ndao, Y. Peles, M.K. Jensen, Effects of pin fin shape and configuration on the single-phase heat transfer characteristics of jet impingement on micro pin fins, Int. J. Heat Mass Transfer 70 (2014) 856–863.